Thermographic Characterization of Impact Damage in SiC/SiC Composite Materials

Laura M. Cosgriff[a], Ramakrishna Bhatt[b], Sung R. Choi[c], Dennis S. Fox[d]
[a]Cleveland State University, Cleveland, Ohio; [b]U.S. Army Aviation Systems Command;
[c]Univesity of Toledo; [d]NASA Glenn Research Center

ABSTRACT

SiC/SiC composite materials targeted as turbine components for next generation aero-engines are being investigated at NASA Glenn Research Center. In order to examine damage mechanisms in these materials, SiC/SiC coupons were impacted with 1.59 mm diameter steel spheres at increasing velocities from 115 m/s to 400 m/s. Pulsed thermography, a nondestructive evaluation technique that monitors the thermal response of a sample over time, was utilized to characterize the impact damage. A thermal standard of similar material was fabricated to aid in the interpretation of the thermographic data and to provide information regarding thermography system detection capabilities in 2.4 mm thick SiC/SiC composite materials. Flat bottom holes at various depths with aspect ratios greater than 2.5 were detectable in the thermal images. In addition, the edges of holes at depths of 1.93 mm into the sample were not as resolvable as flat bottom holes closer to the surface. Finally, cooling behavior was characterized in SiC/SiC materials and used to determine impact damage depth within an 8.5% error of a known depth.

Keywords: Nondestructive evaluation, thermography, ceramic matrix composites, impact damage

INTRODUCTION

SiC/SiC composite materials are candidate materials for turbine components, such as blades, combustor liners, and nozzle vanes, due to their high temperature strength properties [1]. Water vapor, which causes surface oxidation and recession in SiC/SiC composite materials, is a by-product of the combustion process. To protect the composite from the effects of the water vapor, an environmental barrier coating (EBC) is necessary. Impact damage to the EBC influences its ability to protect the SiC/SiC substrate material in addition to reducing the strength properties of components made from these materials [2]. Therefore, it is necessary to develop nondestructive evaluation (NDE) methods to detect and characterize impact damage in SiC/SiC composite materials with and without EBCs for material development and future inspection purposes. The complex nature of the composite weave and the amount of porosity in ceramic matrix composites makes investigation with ultrasonic methods extremely challenging. In addition, full scale components require immersion in water for ultrasonic c-scan imaging. Conventional x-ray methods are not able to detect planar defects, such as delaminations, that occur due to impact. Micro-focused computed tomography has been useful in detecting damage depth in small SiC/SiC composite samples [2]. However, computed tomography has significant limitations with respect to inspection time, costs, and sample size. These limitations necessitate the research and improvement of other inspection methods, such as pulsed thermography, for SiC/SiC composite materials.

Pulsed thermography has many advantages over conventional NDE methods [3-9]. It is a fast, noncontact method that can detect subsurface defects over wide areas. In addition, the method is capable of measuring defect depths provided a proper calibration standard is available. Damage detection with pulsed thermography is based on the principle that heat flow in a material is altered by the presence of subsurface discontinuities, such as delaminations and voids [3-9]. In this technique, the surface of a component is heated with an instantaneous, uniform pulse of light. The heat is absorbed at the surface and flows toward the backside of the material. Disruptions in heat flow, due to subsurface discontinuities, result in localized surface temperature variations which are detected with an infrared camera. The method has proven to be effective for many applications, including the detection of impact damage in thick composite laminate materials [4].

The long term objective of this research is to develop and improve a thermographic technique to detect and characterize impact damage in uncoated and EBC coated SiC/SiC composite materials. The purpose of the research presented here is to investigate damage detection and characterization capabilities of pulsed thermography in the substrate material,

without the protective layer of the EBC. Uncoated SiC/SiC samples were impact tested with 1.59 mm diameter steel ball projectiles at impact velocities ranging from 115 m/s to 400 m/s. The relationship between impact velocity and damage in SiC/SiC material as detected by thermography was examined. In order to determine the depth of impact damage, a thermal standard with flat bottom holes of varying diameters and depths from the surface was fabricated. The thermal standard also provided information about the detection capabilities of the thermography system with 2.4 mm thick SiC/SiC composite material. To understand defect resolution in SiC/SiC materials, a thermal modulation transfer function technique, which considers the relationship between the image contrast and defect depth, was utilized in conjunction with the thermal standard [5-6]. To quantify the depth of damage in impacted samples, the cooling behavior in regions with and without flat bottom holes was analyzed. Then, the information acquired from the depth analysis was used to demonstrate how to determine the depth of damage on previously collected thermal data from an impacted sample.

PULSED THERMOGRAPHY

The commercially available pulsed thermography system utilized in this study is a full field nondestructive evaluation technique for detecting subsurface flaws and material variations [3-8]. Analysis of the ideal thermal response signal is based on the mathematical expression for surface temperature, T, of a specimen subjected to an instantaneous heat pulse,

$$T = \frac{Q}{e(\pi t)^{0.5}}$$

where Q is the input energy, t represents time, and e denotes the effusivity of the sample [4-8]. Effusivity, a measure of the ability of a material to increase its temperature due to a given energy, is the square root of the product of thermal conductivity, density, and specific heat of the material of interest. The natural log of the above equation is

$$\ln(T) = \ln(\frac{Q}{e}) - 0.5\ln(\pi t)$$

In the logarithmic domain, the thermal response is linear with a slope of -0.5 [3-8]. The time at which the function deviates from this linear behavior corresponds to the transition from ideal one-dimensional conductive cooling behavior to two-dimensional, lateral heat flow due to the presence of a subsurface defect. After calibrating the system to a known defect depth, the time of departure from linear cooling behavior can be used to measure unknown defect depths [6-7].

The logarithmic time dependence of each pixel in a thermal image can be approximated by an n^{th}-order polynomial function of the form,

$$\ln(T(t)) = \sum_{i=0}^{N} a_i [\ln(t)]^i$$

After the coefficients, a_i, of the relationship are calculated for each pixel, the original thermal image is reconstructed based on the relationship

$$T(t) = \exp\left[\sum_{i=0}^{N} a_i [\ln(t)]^i\right]$$

The reconstructed data offers many advantages, such as a reduction of noise, an optimization of storage and data handling requirements, and allowing for the calculation of derivatives to provide additional or more easily interpreted information [8]. Original time domain and first derivative images are presented in this paper.

EXPERIMENTAL

1. Material Specifications

The impact samples, in the forma of tensile dog bone samples, were sectioned from Sylramic-iBN SiC fiber-reinforced SiC matrix composite panels which were fabricated by a slurry-casting, melt infiltration method as reported in the

reference [9]. This composite was an 8 ply, 0/90 woven SiC/SiC composite. The 2.4 mm thick samples, with dimensions of 150 mm (5.91 in) by 13 mm (0.51 in) with a 10 mm (0.39 in) wide gauge region, were impacted in an air gun facility at room temperature and 1316°C with 1.59 mm diameter chrome steel balls at velocities ranging from 115 m/s to 400 m/s. The specimens were partially supported at the specimen ends in a specimen holder for the impact.

The thermal standard with flat bottom holes, shown in figure 1, was manufactured similar to the manufacturing of SiC/SiC composites impacted in this study. The dimensions of the standard were 152.4 mm (6 in) by 101.6 mm (4 in) by 2.4 mm (0.09 in). Flat bottom holes of varying diameters and depths were machined into the thermal standard to simulate discontinuities, such as delaminations and voids. Damage detection by pulsed thermography is governed not only by the diameter, or width, of a given defect, but its depth from the interrogation surface. Therefore, each hole has a unique aspect ratio, the ratio of the diameter to the depth from the surface, which is shown in parentheses on the schematic in figure 1. In general, defects with aspect ratios less than 2 are not detectable with pulsed thermography in composite materials [3]. However, this standard has defects with aspect ratios ranging form 0.3 to 27.1 for the sake of completeness. The standard was made so that all the flat bottom holes in a common column were at the same depth (0.35 mm, 0.9 mm, 1.32 mm, or 1.93 mm) from the interrogation surface, shown above the respective columns. The depth of the flat bottom hole refers to the remaining thickness of composite. The holes in a common row had the same diameter (0.5 mm, 2.4 mm, 4.8 mm, 7.9 mm, and 9.5 mm), which is shown to the right of the image.

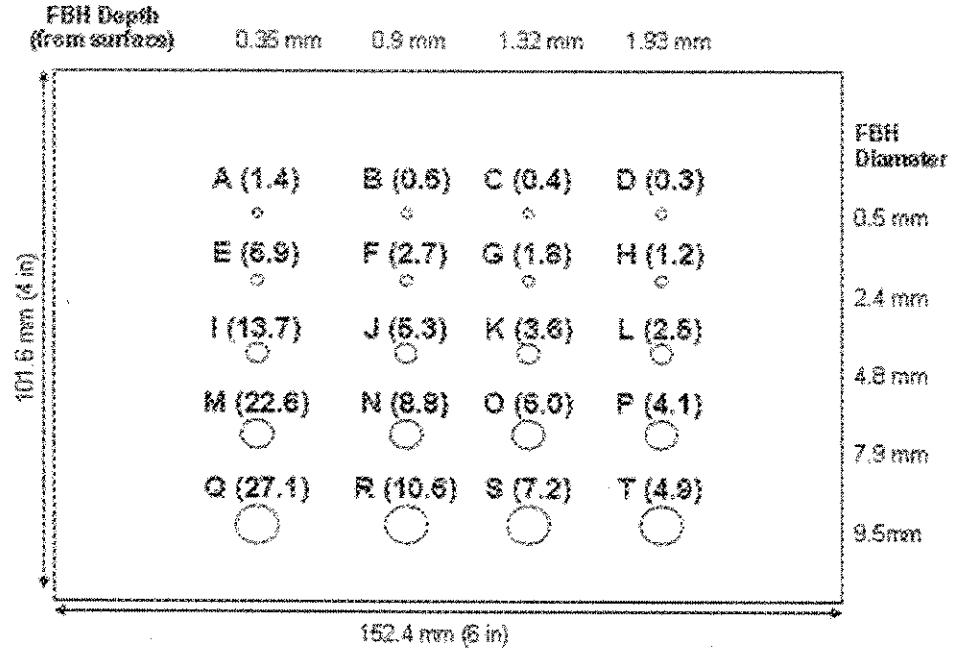

Figure 1. Schematic of the thermal standard with flat bottom holes machined from the backside. Above each hole is an alphabetical label with its aspect ratio in parentheses for reference purposes.

2. Pulsed Thermography Setup

The experimental setup for pulsed thermography is depicted in figure 2. Two high energy xenon flash lamps, placed to provide a relatively uniform heat distribution across the surface of a component, produce a 1.8 kJ flash with a 2 ms duration. A high speed, 640 by 512 InSb focal plane array infrared camera monitors the thermal response of the component of interest over time. A smaller portion of the focal plane array may be utilized to increase the acquisition rate. For the thermal standard, a 80 by 128 portion of the full array was utilized for a frame acquisition rate of 613 Hz. As the impact specimens were tested and destroyed prior to designing the thermal standard, a less optimum acquisition rate of 409 Hz with a 160 by 128 portion of the full array was utilized. Samples were placed in front of the thermal camera so the gauge region of each sample filled the active focal plane. Flash initiation, data collection, storage, and processing were performed with a commercially available software package loaded onto the acquisition computer. The software acquires a data cube which consists of a sequence of thermal images starting just prior to the flash event. Each

image represents the thermal response at a different point in time. The data cube acquired from the impacted samples and the thermal standard consisted of 185 images (or a time length of 0.45 secs) and 1226 images (or a time length of 2 secs), respectively.

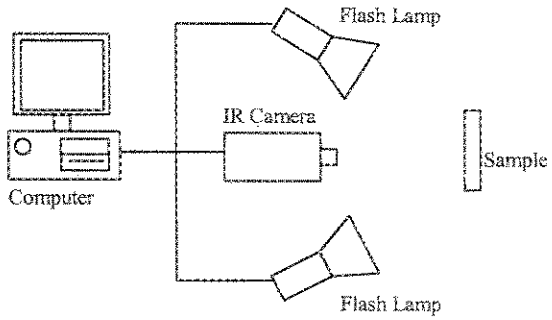

Figure 2. Pulsed thermography experimental setup.

RESULTS

1. Damage progression due to increasing impact velocity

Figure 3 illustrates the progression of damage due to increasing velocity as detected optically from the impacted side (a) and the back side (b) of each impacted sample. The set of samples examined in this section were impact tested at 1316° C. It is apparent from the figure that as impact velocity increased, damage increased. For the lower impact velocities from 115 to 220 m/s, damage approximately the diameter of the projectile is visible. From the impact surface, it appears that some spalling occurs at 300 m/s. At velocities of 325 m/s and above the projectile punctured through the sample with some additional spalling occurring on the back surface. In general, the optical images suggest that significant damage into the bulk of the material is not initiated for impact velocities below 300 m/s.

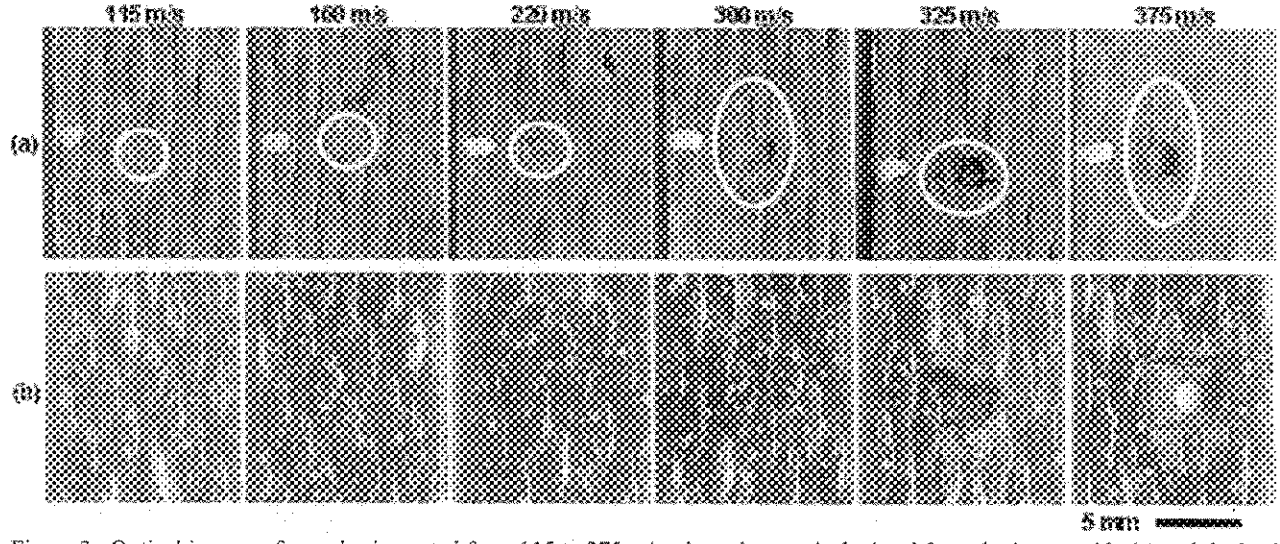

Figure 3. Optical images of samples impacted from 115 to 375 m/s where damage is depicted from the impact side (a) and the back side (b). A white mark to the left of each impact was used to identify the impact location.

Thermal derivative images, illustrating the progression of damage as detected by thermography from the impacted side (a) and the back side of each sample (b), are shown in figure 4. The thermal derivative images represent the rate of temperature change at the sample surface, with black depicting a slower rate of temperature change due to heat being trapped above a subsurface defect, such as a delamination. The derivative images from the impacted SiC/SiC samples are depicted since they provide better contrast than the relative temperature images. Each individual derivative image was chosen based on the levels of contrast between the damaged and undamaged zones of each sample. For the lowest

impact velocities of 115 m/s, damage was not detected with thermography as the damage was masked by the surface roughness of the sample. Although the contrast levels are difficult to discern, the surface impact damage was somewhat detectable for the impact velocity of 160 m/s. At 220 m/s, the surface damage was detected on the impact side. In addition, a delamination, which was not detected optically, was detected from the back side of the sample. At 300 m/s, delaminations beyond the visible damage are detected on the impact side and the back side of the sample. For impact velocities of 325 m/s and 375 m/s, damage beyond the visible damage was also detected. Thermally, there appears to be less damage at these higher velocities. However, the projectile punctured through the thickness of these samples.

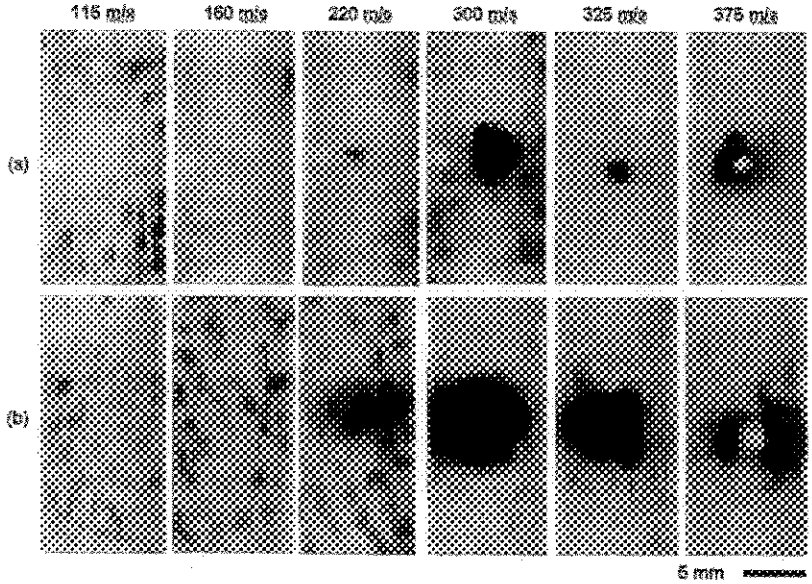

Figure 4. Thermal derivative images of samples impacted from 115 to 375 m/s where damage is depicted from the impact side (a) and the back side (b) with black representing damage due to a slow rate of temperature change.

Figure 5 plots width of damage as detected optically and thermally against the impact velocity. In general, the width of damage detected with thermography is greater than the damage that can be detected optically, excluding the surface damage at 115 and 160 m/s. The width of damage detected from the back side with thermography is significantly larger than damage detected optically or with thermography from the impacted side for impact velocities above 220 m/s. Damage is closer to the back surface than the impacted surface of the sample. However, components made from this material may be accessible from a single side only. This observation illustrates the need for defining the limits of detection in SiC/SiC composite material and optimizing the capture of thermal data in this material. In addition, the damage depth information needs to be acquired from the thermal data.

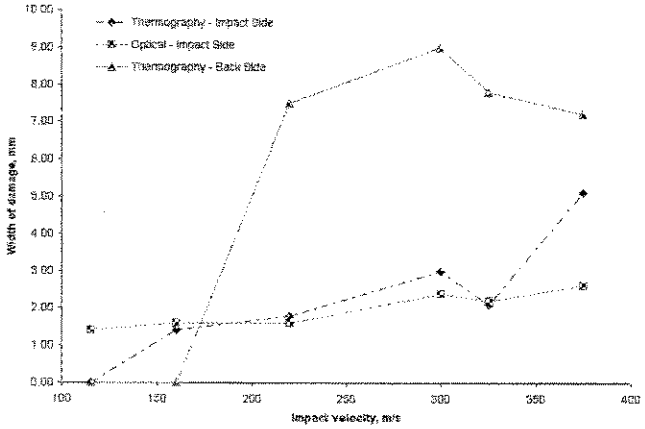

Figure 5. Width of damage for each impact velocity as detected optically from the impacted surface and thermally from the impacted surface and the back surface.

2. Thermal modulation transfer function

Figure 6 shows a series of thermal images of the standard. The white ladder pattern is a match pattern for image processing, since the thermal images were captured over four regions and were assembled together. Flat bottom holes closer to the interrogation surface appear earlier in time so that qualitatively, flat bottom hole depth can be observed. Also, all the holes that were 0.35 mm from the interrogation surface were detected, including the 0.5 mm diameter hole designated as A, which appears very faintly in figure 6a and b. Interestingly, this flat bottom hole has an aspect ratio of 1.4 and was not anticipated to be detected. However, the holes with aspect ratios of 1.8 and 1.2, G and H respectively, were not detected. All the holes with aspect ratios above 2.5 were detected. However, hole L with an aspect ratio of exactly 2.5, and depth 1.93 mm from the surface, is slightly more difficult to detect. Its edges are much less defined than the holes that were closer to the surface. In general, the deeper holes that appear later in time are less defined than the flat bottom holes with similar aspect ratios that are closer to the surface.

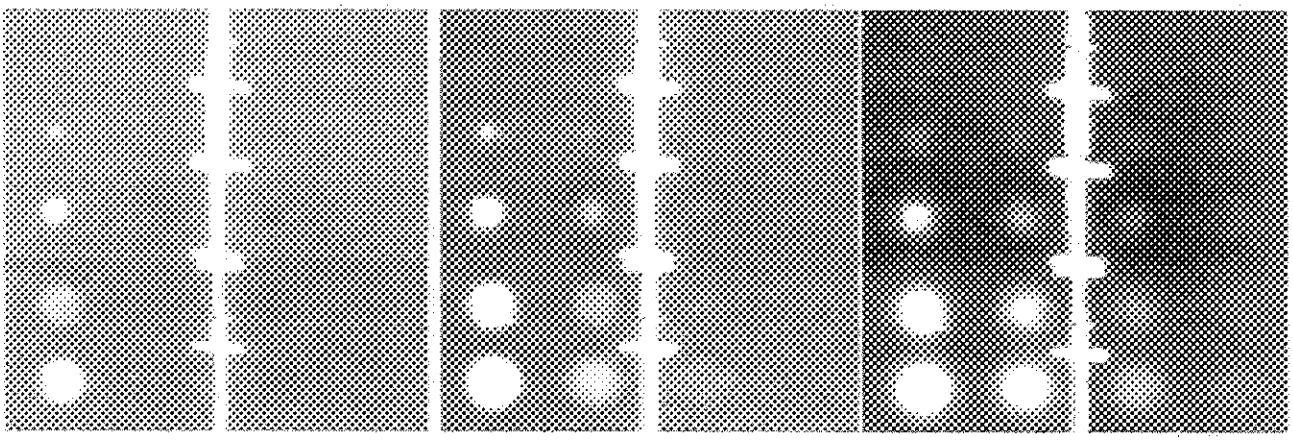

Figure 6. Thermal images at 7 msecs (a), 18 msecs (b), and 70 msecs (c) after the flash event.

To aid in quantifying the minimum level of defect resolution in the SiC/SiC material with the pulsed thermography system described, the thermal modulation transfer function (TMTF) method introduced by Shepard [5-6] was utilized. Traditionally, the modulation transfer function is used to evaluate optical imaging system performance. The TMTF considers the relationship between the image contrast (or modulation) and the depth of the defect. The modulation for each flat bottom hole was calculated using the mathematical equation,

$$M_i = \frac{\sum \left[I_j(center) - I_j(space)/2 \right]_i}{\sum \left[I_j(center) + I_j(space)/2 \right]_i}$$

where I represents the image intensity. The peak intensity occurred at the center of each flat bottom hole. Two lower intensities were taken one diameter from the center. Figure 7 shows the modulation for flat bottom holes plotted as a function of 1 divided by the depth. The trend line in the plot represents a least squares fit of a straight line to the data with R^2=0.9785, suggesting that defect depth is a good indicator of the resolvability of a defect. Flat bottom holes with aspect ratios below 1.8 were not included in the plot as they were not expected to be detectable. In addition, most of these holes had diameters of 0.5 mm which introduces a source of resolution error independent from thermal capabilities since each individual pixel represents a width and height of 0.26 mm. Flat bottom hole E was considered an outlier due to anomalous behavior from unexpected irregularities in the material and was not included.

For this material system, the resolution threshold was approximately 8% modulation based on modulation values from regions of the thermal standard without flat bottom holes. This value, which corresponds to approximately 1.6 mm from the interrogation surface, provides a rough gauge as to resolvable defect depths for this material system. It is noteworthy that the thickness to depth (L/d) ratio for holes L, P, and T, was 1.2. The modulation for these holes falls below the modulation threshold, indicated as a dashed line in figure 7. Holes K and F, with aspect ratios of 3.6 and 2.7, had L/d ratios of 1.8 and 2.7, respectively. These holes are above the modulation threshold. This observation illustrates the effect that the relationship between sample thickness and hole depth has on the resolution of flat bottom holes.

Two-dimensional, lateral heat flow is the dominant cooling mechanism at the back surface. Defects near the back surface are less resolvable as there is less of a transition from predominantly one-dimensional heat flow to two-dimensional heat flow. Hence, the edges of flat bottom holes located closer to the interrogation surface, such as the holes at depths of 0.9 mm and 1.32 mm, with lower aspect ratios were better resolved than deeper holes with higher aspect ratios.

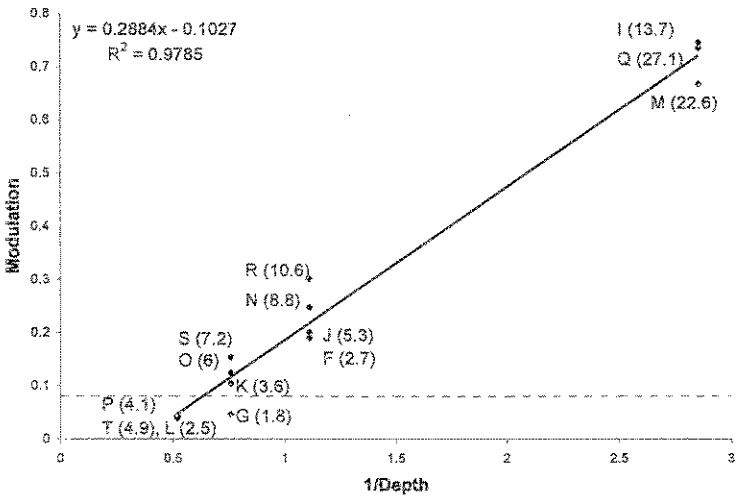

Figure 7. Modulation plotted against 1/depth with hole designations and aspect ratios next to each plot point.

3. Depth of damage

The thermographic standard was essential for estimating the depth of damage in SiC/SiC materials. The methods for determining depth of damage were developed by Shepard [6]. Figure 8 shows the logarithmic cooling behavior of three regions from the standard compared to a reference area: (a) flat bottom hole R located 0.90 mm below the surface, (b) S located 1.32 mm below the surface, and (c) T located 1.93 mm below the surface. The reference region represents the average response from a 25 by 25 pixel area without holes. For the regions compared to the reference region, a 3 by 3 pixel area was taken in the center of each flat bottom hole. The time at which the dominant cooling mechanism changes from one-dimensional heat flow to two-dimensional, lateral heat flow is referred to as the time of departure and is labeled t_d in the plots. The cooling behavior for all three locations is identical to the reference region until t_d. The time of departure increases as the location of the flat bottom holes deepens into the material. For the flat bottom holes at depths of 0.35 mm below the surface, t_d was not detected as the sampling rate associated with the camera was too slow to capture the early departure time in this material.

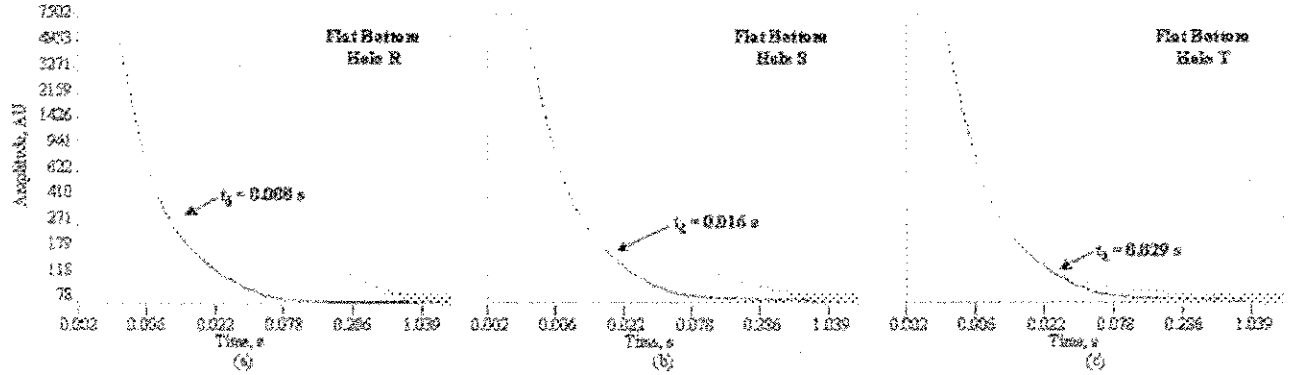

Figure 8. Thermal cooling behavior in the logarithmic domain for flat bottom holes at depths of (a) 0.90 mm, (b) 1.32 mm, and (c) 1.93 mm below the surface plotted against a reference region. The reference region is represented by the black curve, while the compared region is represented with gray.

Figure 9 shows a plot of the average t_d for the flat bottom holes with depths of 0.9 mm, 1.32 mm, and 1.93 mm from the interrogation surface. A straight line with a R^2 value of 0.9991 is fit to the three points. Hence, the depth of damage can be estimated in components made from SiC/SiC materials based on the observed t_d. An illustration of the application of this data to an impacted sample is presented in the next section. Although near surface damage is definitely detectable, it should be noted that damage depths very near the surface may not be able to be determined with accuracy.

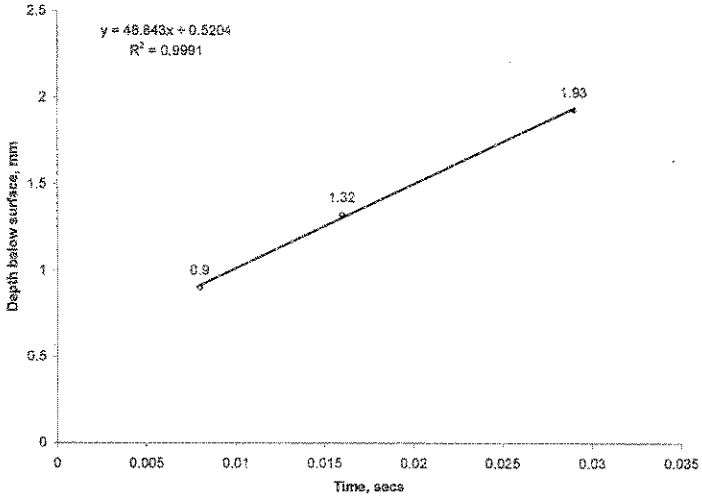

Figure 9. Plot of the average t_d for flat bottom hole depths of 0.9 mm, 1.32 mm, and 1.93 mm from the surface with a straight line fit through the points.

4. Depth of damage tools applied to impacted sample data

To illustrate how the depth of damage analysis may be applied, the information acquired from the standard was compared to thermal data acquired from an impacted SiC/SiC sample with known damage. The sample examined here was impacted at room temperature. Figure 10 shows a thermal image of the impacted sample with the cooling curves for a 13 by 13 pixel area averaged reference region and a delaminated 1 by 1 pixel area. The sample, impacted at 300 m/s, had clearly identifiable damaged and undamaged regions in the thermal image. As shown in the cooling curve, the time of departure from the reference region is 0.031 seconds. Based on the equation derived from the analysis of the SiC/SiC standard shown in figure 9, this time corresponds to a depth of 2.03 mm from the surface, which has an 8.5 percent error when compared to the depth of the delamination of 1.87 mm, as measured from a computed tomography image. The commercially available thermography analysis software used in this study has a calibration tool to be used with a calibration standard, like the standard from this study. After calibration with the standard, damage depth can be measured in SiC/SiC composite materials with thicknesses of approximately 2.4 mm.

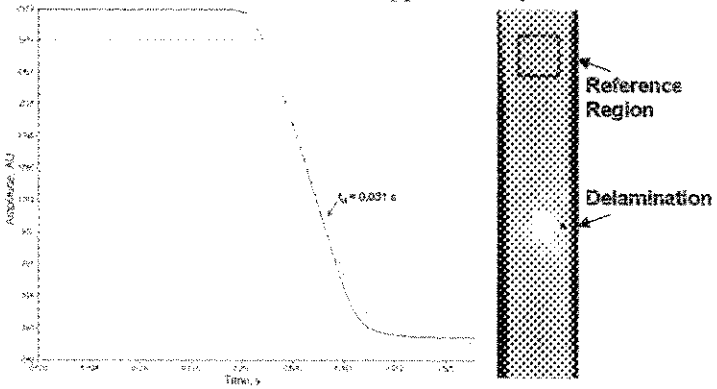

Figure 10. Cooling behavior for an impacted SiC/SiC sample where the reference region represents a 13 by 13 average pixel area and the damaged region is a 1 by 1 pixel region.

The 8.5 percent error between the computed tomography measurement and the estimated depth from the cooling curve analysis may be due to the difference in acquisition parameters between the standard and the impacted sample. The thermal data from the impacted sample was acquired prior to manufacturing the thermal standard with a sampling rate of 409 Hz (capturing an image every 2.4 msecs). The sampling rate for the standard was 613 Hz (capturing a frame every 1.6 msecs). The difference in time resolution can cause a difference in time of departure from the reference curve. It should be noted that there is a region of saturation, or flattening, in the cooling curve from 0 to 20 msecs. Saturation is due to temperature intensity values that are beyond the IR camera's range and typically occurs immediately after the flash. Saturation does not introduce another source of error. Surface irregularities can cause saturation to be observed. However, the cooling rate and pattern will not vary due to this saturation. Therefore, the comparison between the data acquired from the impacted sample and the thermal standard is still valid. Many of these saturation issues have been resolved since the thermal data from the impacted sample was captured.

DISCUSSION

The results presented here are valid for uncoated SiC/SiC composite materials with thicknesses of approximately 2.4 mm. The thermal modulation transfer analysis illustrated that the dominant heat flow mechanism of two-dimensional heat flow at the back surface interferes with the resolution of discontinuities near the back surface. It is probable that damage at depths of approximately 1.9 mm from the interrogation surface would be better resolved and detected in thicker samples. Any additional changes to the structure or geometry of this material will likely change the thermal response. For example, the addition of environmental barrier coatings will require new standards and analysis as the thermal response of the material system will change.

Flat bottom holes represent a best case scenario with respect to detection. When a defect is backed by additional material, as in the case of a delamination, damage with similar aspect ratios may be more difficult to resolve and detect. Meola [10] observed that the thickness of a defect has influence on its detectability with thermal methods. So, defects near the back surface with additional material backing may not be detected from the front (impacted) surface. For example, delaminations 1.93 mm from the front surface may not be detected in these SiC/SiC composites, since the flat bottom holes at this depth were the least resolvable in terms of contrast. Additional material beyond the delamination may make those types of defects undetectable. However, the flat bottom holes are more representative of the type of thermal response that may occur with spalling. So, spalling may be detectable for depths of 1.93 mm provided the aspect ratio is above 2.5, meaning the diameter of the spalled region is greater 5 mm at a depth of 1.93 mm. The thermal standard gives a good reference point, in terms of aspect ratio, as to defect detection expectations in these composite materials. Flat bottom holes with aspect ratios above 2.5 were detected in SiC/SiC material with thermography. Even though the flat bottom holes represent a best case of detection scenario, the cooling curve analysis for depth measurement will not differ when comparing the thermal standard to a damaged sample. The time of departure from reference behavior should not change with the addition of material to the backside of a defect.

These results illustrate some challenges of defect detection in SiC/SiC composite materials by pulsed thermography. As illustrated in figure 5, surface damage on the level of the surface roughness of the weave was not readily detected with thermography. In addition, damage near the back surface of the composite, although detectable for aspect ratios above 2.5, is not easily resolved due to the two-dimensional heat flow being the dominant heat flow mechanism at the back surface. The lack of resolution for defects near the back surface means that the measurement of width or diameter for a defect may have a significant amount of error associated with it. Depth measurements for near surface flat bottom holes also proved challenging. The SiC/SiC composite material cools at such a high rate, that the time of departure for the flat bottom holes closest to the surface (0.35 mm) was not captured. The highest capture rate the thermal camera from this study was capable of utilizing, without significantly degrading the images, was 613 Hz. There are commercially available IR cameras that are capable of capturing at higher sampling rates that may be able to provide better depth measurements for near surface defects. Also, with respect to delaminations existing at multiple depths in a local thickness, thermography will detect only the defect nearest the interrogation surface. Heat flow will be interrupted by the first defect in the thickness. This is particularly important for the types of damage existing in impacted SiC/SiC samples. In addition, the conical shape of the damage induced by impact can make depth measurement somewhat difficult, as the depth can be changing within a single pixel width.

Despite these challenges, pulsed thermography is a viable NDE method for use with large scale components fabricated from SiC/SiC composite materials. There are far more significant challenges associated with inspecting SiC/SiC composite materials with conventional NDE techniques due to the types of defects that are of interest, the composite weave and porosity issues. Ultrasonic signals for immersion c-scans are typically attenuated by the composite weave and porosity. Conventional x-ray methods are not sensitive to the planar defects that are typical of impact damage. Computed tomography has limitations concerning time costs and component size. Pulsed thermography outperforms these techniques in terms of contact requirements, speed of data acquisition and analysis, and sensitivity to subsurface, planar defects.

CONCLUSION

Impact damage in SiC/SiC composite materials targeted for high temperature environments was investigated and characterized with pulsed thermography. Damage that went undetected optically was detected with thermography at velocities as low as 220 m/s. A thermal standard was fabricated for the purpose of determining defect resolution limits and impact damage depth in these materials. Although detectable in the thermal image sequence, the edges of flat bottom holes with depths 1.93 mm from the interrogation surface were not readily resolved due to their proximity to the back surface. Holes with aspect ratios above 2.5 were detectable in the thermal image sequence for all depths from the interrogation surface. Cooling behavior was successfully characterized in SiC/SiC materials and applied to determine impact damage depth within an 8.5% error of the known depth.

In addition to impact damage, these results can be utilized to characterize manufacturing defects in samples and components made from SiC/SiC materials with thicknesses of approximately 2.4 mm. This research represents a portion of a larger effort to develop and improve pulsed thermography for detection and characterization of impact damage in uncoated and EBC coated SiC/SiC composite materials. Research is continuing with the investigation of impact damage with pulsed thermography in EBC coated SiC/SiC composite materials.

REFERENCES

1. David Brewer. "HSR/EPM combustor materials development program." *Materials Science and Engineering* A261 (1999): 284-291.
2. R.T. Bhatt, S.R.Choi, L.M. Cosgriff, D. Fox, and K.N. Lee. "Foreign Object Damage Resistance of Uncoated SiC/SiC Composites" *Proc. Fifth International Conference on High Temperature Ceramic Matrix Composites (HTCMC-5), Sept 12-16, 2004, Seattle, WA.* ACerS
3. *Nondestructive Testing Handbook, Volume 3, Infrared and Thermal Testing*, eds. Xavier P.V. Maldague and Patrick O. Moore. Columbus: ASNT, 2001.
4. Steven M. Shepard, James R. Lhota, Tasdiq Ahmed, and Yu Lin Hou, "Thermographic Inspection of Composite Structures," SAMPE Journal, Vol. 39, No. 5, 2003, pp 53-59.
5. Steven M. Shepard, James R. Lhota, Bruce A. Rubadeux, and Tasdiq Ahmed, "Onward and inward: Extending the limits of thermographic NDE," *Proc. SPIE Thermosense XXII,* 2000, Vol. 4020, p. 194.
6. S. M. Shepard, B.A. Rubadeux, and T. Ahmed, "Automated Thermographic Defect Recognition and Measurement," AIP Conf. Proc., Vol. 497, Issue 1, 1999, pp 373-378.
7. S.M. Shepard, J.R. Lhota, T. Ahmed, B.A. Rubadeux, and D. Wang, "Quantification and Automation of Pulsed Thermography NDE," *Proc. SPIE Nondestructive Evaluation of Materials and Composites V*, Vol. 4336, Bellingham, Washington, SPIE, March 2001, pp. 73 – 78.
8. Richard E. Martin, Andrew L. Gyekenyesi, and Stephen M. Shepard, "Interpreting the Results of Pulsed Thermography Data," *Materials Evaluation*, Vol. 61, No. 5, 2003, pp. 611 – 616.
9. S. K. Lau, S. J. Calandra, and R. W. Ohnsorg, US Pat. #5,840,221, (1998).
10. Carosena Meola, Giovanni Maria Carlomagno, and Luca Giorleo, "Geometrical Limitations to Detection of Defects in Composites by Means of Infrared Thermography," Journal of Nondestructive Evaluation, Vol 23, No. 4, December 2004, pp 125- 132.